

BFKL pomeron propagator in the external field of the nucleus

M.A.Braun, A.N.Tarasov
S.Peterburg State University, Russia

February 24, 2024

Abstract

It is shown by numerical calculations that the convoluted QCD pomeron propagator in the external field created by a solution of the Balitsky-Kovchegov equation in the nuclear matter vanishes at high rapidities. This may open a possibility to apply the perturbative approach for the calculation of pomeron loops.

1 Introduction

In the QCD, in the limit of large number of colours, strong interaction at high energies is mediated by the exchange of BFKL pomerons, which interact via their splitting and fusion. In the quasi-classical approximation for photon (hadron)-nucleus scattering the relevant tree (fan) diagrams are summed by the well-known Balitsky-Kovchegov (BK) evolution equation [1, 2, 3]. For nucleus-nucleus scattering appropriate quasi-classical equations were derived in [4, 5]. In both cases pomeron loops were neglected. This approximation can be justified if the parameter $\gamma = \lambda \exp \Delta_P y$ is small, with y the rapidity and Δ_P and λ the pomeron intercept and triple pomeron coupling. Then for a large nuclear target, such that $A^{1/3}\gamma \sim 1$, the tree diagrams indeed give the dominant contribution and loops can be dropped. However with the growth of y the loop contribution becomes not small and this approximation breaks down.

Direct calculation of the loop contribution seems to be a formidable task for the non-local BFKL pomeron. Simplest loops have been studied in several papers for purely hadronic scattering [6, 7, 8]. In particular in [8] it has been found that pomeron loops become essential already at rapidities of the order $10 \div 15$. They shift the position of the pomeron pole to the complex plane and thus lead to oscillations in cross-sections. However with the growth of energy loop contributions begin to dominate and one needs to sum all of them. There have been many attempts to do this in the framework of the so-called reaction-diffusion formulation of the QCD dynamics and the following correspondence with the statistical approach [9, 10, 11, 12, 13, 14] (see also a review [15] and references therein). Unfortunately concrete results could be obtained only with very crude approximations for the basic BFKL interaction and the stochastic noise in the statistical formulation. The conclusions of different groups are incomplete and contradictory. So in [14] it was found that the geometric scaling following from the BK equation was preserved with loops taken into account, although going to the black disc limit was much slower. On the contrary in papers based on the analogy with statistical physics (see [13, 15]) it was argued that the BK scaling was

changed to the so called diffusive scaling (with an extra \sqrt{y} in the denominator of the argument) but the speed of achieving the black disk limit was essentially unchanged.

In our previous study of pomeron loops [16] we considered a much simpler model with the local supercritical pomeron in the Regge-Gribov formalism. Instead of trying to solve the model for the purely hadronic scattering we considered the hadron-nucleus scattering and propagation of the pomeron inside the heavy nucleus target. Moreover to avoid using numerical solution of the tree diagrams contribution with diffusion in the impact parameter, we concentrated on the case of a constant nuclear density, which allowed to start with the known analytical solutions. We have found that the nuclear surrounding transforms the pomeron from the supercritical one with intercept $\epsilon > 0$ to a subcritical one with the intercept $-\epsilon$. Then Regge cuts, corresponding to loop diagrams, start at branch points located to the left of the pomeron pole and their contribution is subdominant at high energies. As a result, the theory acquired the properties similar to the Regge-Gribov one with a subcritical pomeron and allows for application of the perturbation theory. In [16] we expressed our hopes that a similar phenomenon might occur in the QCD with BFKL pomerons.

In this note we demonstrate that such hopes are possibly founded. We consider the pomeron propagator in the nuclear field and give arguments that, similar to the local Regge-Gribov case, it vanishes at large rapidity distances. We stress that at present we are unable to give the full proof for this behaviour. Our study is based on numerical calculations. This makes us to choose a relatively small subset of initial conditions out of the complete set necessary for the study of the pomeron propagator. Our numerical results show that, with the chosen set of initial conditions, this pomeron propagator vanishes at large rapidity distances. This result may serve as a starting point for the study of loops and can be directly applied for double inclusive cross-sections in the nucleus-nucleus scattering.

2 Local pomeron in the nuclear field

To make clear our motivation and goals we start with reviewing our treatment of a simpler model, the local reggeon field theory (LRFT) with a supercritical pomeron and triple pomeron interaction. The following passage to the non-local BFKL pomeron will not introduce ideologically new moments, although greatly complicates the technique.

The LRFT model is based on two pomeron fields $\Phi(y, b)$ and $\Phi^\dagger(y, b)$ depending on the rapidity y and impact parameter b , with a Lagrangian density [17]

$$L = L_0 + \lambda \Phi^\dagger \Phi (\Phi + \Phi^\dagger) + g \rho \Phi^\dagger. \quad (1)$$

Here the free Lagrangian density is

$$L_0 = \Phi^\dagger \left(\frac{1}{2} \overset{\leftrightarrow}{\partial}_y - \alpha' \nabla_b^2 + \epsilon \right) \Phi \equiv \Phi^\dagger S \Phi, \quad (2)$$

where ϵ is the intercept minus unity and α' is the slope. The source term describing interaction with the nuclear target at low energies is

$$g \rho(y, b) = g A T_A(b) \delta(y), \quad (3)$$

where g is the pomeron-nucleon coupling constant and $T(b)$ the profile function of the nucleus. For a supercritical pomeron $\epsilon > 0$ and $\lambda < 0$.

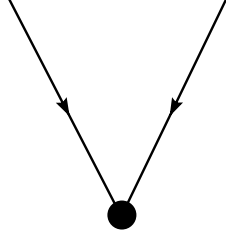


Figure 1: The new vertex for two-pomeron annihilation, which appears after the shift in field Φ

Solution of the classical equation of motion for field Φ^\dagger is $\Phi_0^\dagger = 0$ and the classical equation for Φ becomes

$$\partial_y \Phi = -\alpha' \nabla_b^2 \Phi + \epsilon \Phi + \lambda \Phi^2, \quad (4)$$

with an initial condition

$$\Phi(y=0) = gT_A(b). \quad (5)$$

Equation (4) describes evolution of the pomeron field in rapidity and its diffusion in the impact parameter inside the nucleus. We denote the solution of the classical equation of motion (4) with the initial condition (5) as $\Phi_0(y, b)$.

To go beyond the classical approximation and thus study loops one makes a shift in the quantum field Φ :

$$\Phi(y, b) = \Phi_0(y, b) + \Phi_1(y, b) \quad (6)$$

and reinterprets the theory in terms of quantum fields Φ_1 and Φ^\dagger . In the Lagrangian terms linear in Φ^\dagger vanish due to the equation of motion for Φ and we obtain

$$L = \Phi_1(S + 2\lambda\Phi_0)\Phi^\dagger + \lambda\Phi_0\Phi^{\dagger 2} + \lambda\Phi_1\Phi^\dagger(\Phi_1 + \Phi^\dagger). \quad (7)$$

This Lagrangian corresponds to a theory in the vacuum with the pomeron propagator in the external field $f(b, y) = 2\lambda\Phi_0(y, b)$

$$P = -(S + 2\lambda\Phi_0)^{-1}, \quad (8)$$

the standard triple interaction and an extra interaction described by the term $\lambda\Phi_0\Phi^{\dagger 2}$. This new interaction corresponds to transition of a pair of pomerons into the vacuum at point (y, b) with a vertex $\lambda\Phi_0(y, b)$, see Fig. 1. The propagator P in the external field is described by a sum of diagrams shown in Fig. 2.

Loops can be formed both by the standard interaction and the new one. In the latter case they are to be accompanied by at least a pair of standard interactions. Simplest loops in the Green function are illustrated in Fig. 3, where it is assumed that the propagators are all taken in the nuclear field f . Note that a loop formed by the standard interaction has the lowest order λ^2/α' and requires renormalization in this model. A loop formed by the new interaction has the lowest order λ^3/α' and is finite.

The quantum part of the amplitude is obtained as a tadpole $g < \Phi_1(y, b) >$. The simplest diagram for it contains one loop and is shown in Fig. 4.

Propagator (8) in the external field $f(y, b) = 2\lambda\Phi_0(y, b)$ satisfies the equation

$$\frac{\partial P(y, b|y'b')}{\partial y} = (\epsilon - \alpha' \nabla_b^2) P(y, b|y', b') + f(y, b) P(y, b|y', b') \quad (9)$$

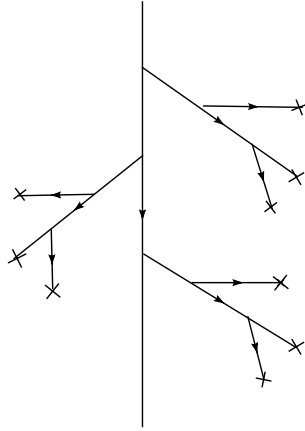


Figure 2: Diagrams summed into the pomeron propagator in the nuclear field

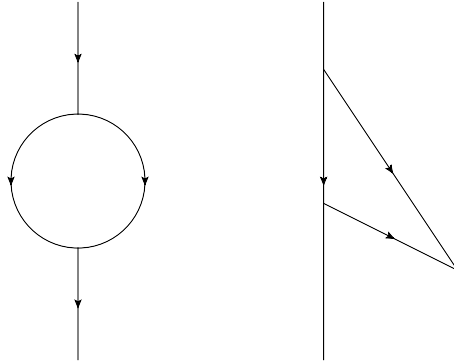


Figure 3: Simplest loop diagrams for the pomeron Green function

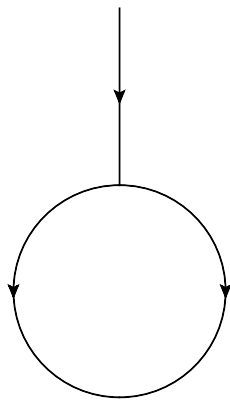


Figure 4: The lowest order diagram for the quantum correction to the scattering amplitude

with the boundary conditions

$$P(y, b|y', b') = 0, \quad y - y' < 0, \quad P(y', b|y', b') = \delta^2(b - b'). \quad (10)$$

In the general case propagator P can only be calculated numerically, just as the external field $f(y, b)$. Its analytic form can be found in two cases [16]: if the slope $\alpha' = 0$ or if one is studying the nuclear matter with the profile function $T_A(b) = T_0$ independent of b . In the second case, relevant for our following studies, the nuclear field becomes independent of b (but dependent on y) and the propagator in this field takes the form

$$P(y, b|y', b') = \frac{1}{4\pi\alpha'(y - y')} \frac{p^2(y')}{p^2(y)} e^{\epsilon(y - y') - \frac{(b - b')^2}{4\alpha'(y - y')}}, \quad (11)$$

where

$$p(y) = 1 - \frac{\lambda g T_0}{\epsilon} (e^{y\epsilon} - 1). \quad (12)$$

Remarkably at $y \rightarrow \infty$ this propagator vanishes as $e^{-(y - y')\epsilon}$. This means that contributions from the loops will be small at large y , so that one can calculate them by the standard perturbation approach.

3 Interacting BFKL pomerons

Now we pass to our main subject, the theory of interacting BFKL pomerons. By its structure it is quite similar to the considered LRFT model. However now the pomeron, apart of the impact parameter b , depends on the relative transversal distance r between the two reggeized gluons out of which it is formed. So it is described by two fields $\Phi(y, r_1, r_2)$ and $\Phi^\dagger(y, r_1, r_2)$ depending on rapidity y and transverse coordinates of the reggeized gluons r_1 and r_2 . The Lagrangian has a general structure similar to (1):

$$L = L_0 + L_I + L_E. \quad (13)$$

Here the free Lagrangian is

$$L_0 = \int d^2r_1 d^2r_2 \Phi^\dagger \nabla_1^2 \nabla_2^2 \left(\frac{\partial}{\partial y} + H_{BFKL} \right) \Phi, \quad (14)$$

where H_{BFKL} is the Hamiltonian for the BFKL pomeron [18]. The triple pomeron interaction is given by

$$L_I = \frac{2\alpha_s^2 N_c}{\pi} \int \frac{d^2r_1 d^2r_2 d^2r_3}{r_{12}^2 r_{23}^2 r_{31}^2} \Phi^\dagger(y, r_1, r_2) \Phi^\dagger(y, r_2, r_3) K_{31} \Phi(y, r_3, r_1) + (\Phi \leftrightarrow \Phi^\dagger), \quad (15)$$

where $r_{ik} = r_i - r_k$ and

$$K_{31} = r_{31}^4 \nabla_3^2 \nabla_1^2. \quad (16)$$

The interaction with the nuclear target is

$$L_E = - \int d^2r_1 d^2r_2 \Phi^\dagger J, \quad (17)$$

where

$$J(y, r_1, r_2) = g A T_A(b) \rho(r_{12}) \delta(y), \quad (18)$$

T_A is as before the profile function of the nucleus and ρ is the colour density of the nucleon.

Our idea is to repeat the procedure applied to the local pomeron as described in the preceding section. First one solves the classical equation for the fields. Its solution for Φ is a sum of all tree diagrams with the pomeron splitting in two. This solution satisfies the BK equation and although not known analytically can be found numerically. At the next step we calculate the quantum correction to this solution (pomeron loops). To this aim we shift the field Φ with a non-zero classical value Φ_0 by this value, passing to the new quantum field $\Phi_1 = \Phi - \Phi_0$, exactly as for the LRFT, and study the theory in terms of fields Φ_1 and Φ^\dagger . This leads to a change in the Lagrangian quite similar to what has been described in the preceding section. In the new theory the propagator is to be taken in the nuclear field. This is achieved by substituting one of the two fields Φ by its classical value Φ_0 in the part of interaction quadratic in Φ . Also in the new theory there appears a new interaction term, obtained when in the part of interaction linear in Φ one substitutes Φ by its classical value.

In this paper we are not attempting at the calculation of loops. We limit ourselves with the starting point of this program: studying the pomeron propagator in the described nuclear field. Our aim is to understand if this propagator vanishes at large rapidities instead of growing in the absence of the field, as it occurs in the LRFT. If it is indeed so then one can hope to calculate loop contributions in the nuclear surrounding perturbatively. Otherwise this surrounding is useless for loop calculations. The BFKL propagator $P(y, r_1, r_2; y', r'_1, r'_2)$ in the nuclear field satisfies the equation

$$\frac{\partial P(y, r_1, r_2)}{\partial y} = \frac{\bar{\alpha}}{2\pi} \int d^2 r_3 \frac{r_{12}^2}{r_{13}^2 r_{23}^2} \left(P(y, r_1, r_3) + P(y, r_2, r_3) - P(y, r_1, r_2) - \Phi(y, r_1, r_3)P(y, r_2, r_3) - \Phi(y, r_2, r_3)P(y, r_1, r_3) \right), \quad (19)$$

where $\bar{\alpha} = \alpha_s N_c / \pi$ and we suppressed the second three variables coordinates y', r'_1, r'_2 on which the equation does not depend. The dependence on them follows from the initial condition:

$$P(y = y', r_1, r_2; y', r'_1, r'_2) = \nabla_1^{-2} \nabla_2^{-2} \delta^2(r_1 - r'_1) \delta^2(r_2 - r'_2). \quad (20)$$

Function $\Phi(y, r_1, r_2)$ in this equation is the solution of the BK equation for the sum of all fan diagrams in the nucleus. It satisfies a non-linear equation

$$\frac{\partial \Phi(y, r_1, r_2)}{\partial y} = \frac{\bar{\alpha}}{2\pi} \int d^2 r_3 \frac{r_{12}^2}{r_{13}^2 r_{23}^2} \left(\Phi(y, r_1, r_3) + \Phi(y, r_2, r_3) - \Phi(y, r_1, r_2) - \Phi(y, r_1, r_3)\Phi(y, r_2, r_3) \right) \quad (21)$$

with the initial condition appropriate for a given nucleus

$$\Phi(y = 0, r_1, r_2) \equiv \Phi_0(r_1, r_2) = 1 - e^{-T_A(b)\rho(r_{12})}. \quad (22)$$

We remind that $b = (r_1 + r_2)/2$, T_A is the conventional profile function of the nucleus and ρ is the colour density of the nucleon.

We shall again study the simple case of the nuclear matter when $T_A(b) = T_0$ is independent of b . Then from the structure of Eq. (21) it follows that Φ is a function of only the relative distance between the gluons $\Phi(y, r_1, r_2) = \Phi(y, r_{12})$. Since the study is only possible numerically, to avoid using the singular initial condition, we shall consider a convolution of $P(y, r_1, r_2; y', r'_1, r'_2)$ with an arbitrary function $\nabla_1^2 \nabla_2^2 \psi(r_1, r_2)$:

$$P(y, r_1, r_2) = \int d^2 r'_1 d^2 r'_2 P(y, r_1, r_2; y', r'_1, r'_2) \nabla_1^2 \nabla_2^2 \psi(r'_1, r'_2). \quad (23)$$

This convolution satisfies the same equation as the propagator itself but at $y = y'$ we have

$$P(y = y', r_1, r_2) = \psi(r_1, r_2). \quad (24)$$

Obviously the properties of the propagator can be studied taking a full set of functions $\psi(r_1, r_2)$.

Note that in the following, for simplicity, we mostly set $y' = 0$. The dependence on the choice of y' will be studied for the forward case and shown to preserve our main conclusions.

4 Forward case

4.1 Main equations

Calculation become especially simple for the forward case when not only Φ but also the convoluted propagator P depend only on the relative distance between the gluons in the pomeron. In this case the equation for P simplifies to

$$\frac{\partial P(y, x)}{\partial y} = \frac{\bar{\alpha}}{2\pi} \int d^2 x_1 \frac{x^2}{x_1^2 x_2^2} \left(P(y, x_1) + P(y, x_2) - P(y, x) - 2\Phi(y, x_1)P(y, x_2) \right). \quad (25)$$

Here we denoted $x = r_{12}$, $x_1 = r_{13}$ and $x_2 = r_{32}$ with $x_1 + x_2 = x$. In the same notation the nuclear field Φ satisfies

$$\frac{\partial \Phi(y, x)}{\partial y} = \frac{\bar{\alpha}}{2\pi} \int d^2 x_1 \frac{x^2}{x_1^2 x_2^2} \left(\Phi(y, x_1) + \Phi(y, x_2) - \Phi(y, x) - \Phi(y, x_1)\Phi(y, x_2) \right), \quad (26)$$

We have to solve this pair of equations with the initial condition for $\Phi(y = 0, x)$ fixed by the properties of the nuclear medium, and the initial condition (24) for $P(y, x)$ taken arbitrary, since we are interested in the propagator in a given nuclear surrounding.

Equation (25) is a linear equation for $P(y, x)$ in contrast to the BK equation. At $y \rightarrow \infty$ $\Phi(y, x) \rightarrow 1$ independent of the chosen initial condition. One may think that at $y \rightarrow \infty$ the behaviour of $P(y, x)$ can be derived from the asymptotic equation

$$\begin{aligned} \left. \frac{\partial P(y, x)}{\partial y} \right|_{y \rightarrow \infty} &= \frac{\bar{\alpha}}{2\pi} \int d^2 x_1 \frac{x^2}{x_1^2 x_2^2} \left(P(y, x_1) + P(y, x_2) - P(y, x) - 2P(y, x_2) \right) \\ &= -P(y, x) \frac{\bar{\alpha}}{2\pi} \int d^2 x_1 \frac{x^2}{x_1^2 x_2^2}. \end{aligned} \quad (27)$$

However the integral on the right-hand side has become divergent (although it converges at finite y). This means that the limit $y \rightarrow \infty$ is more delicate and cannot be taken under the sign of integral over x_1 . And indeed we shall see by numerical calculations that the behaviour of the solution at $y \rightarrow \infty$ is not solely determined by the limiting value of $\Phi(y, x)$ but depends on its behaviour at finite y .

For numerical studies both the BK equation and linear equation (25) in the momentum space are more convenient. Introducing

$$\phi(y, x) = \frac{\Phi(y, x)}{x^2}, \quad p(y, x) = \frac{P(y, x)}{x^2} \quad (28)$$

and then passing to the momentum space we obtain the following equations for $\phi(y, k)$ and $p(y, k)$

$$\frac{\partial \phi(y, k)}{\partial y} = -\bar{\alpha} \left(H_{BFKL} \phi(y, k) + \phi^2(y, k) \right) \quad (29)$$

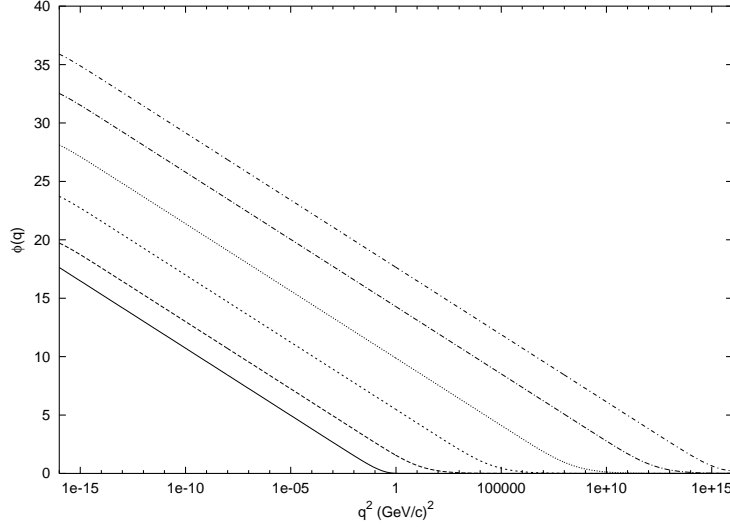


Figure 5: Solution $\phi(y, q)$ of Eq. (29) as a function of q^2 for different of $Y = \bar{\alpha}y$. Curves from bottom to top correspond to $Y = 0, 2, 4, 6, 8$ and 10 .

and

$$\frac{\partial p(y, k)}{\partial y} = -\bar{\alpha} \left(H_{BFKL} + 2\phi(y, k) \right) p(y, k), \quad (30)$$

where

$$H_{BFKL} = \ln k^2 + \ln x^2 - 2(\psi(1) + \ln 2). \quad (31)$$

To study the behaviour of the propagator in the external field ϕ one has to solve this pair of equations with the initial conditions

$$\phi(y, k)_{y=0} = \phi_0(k), \quad p(y, k)_{y=0} = p_0(k), \quad (32)$$

with some fixed ϕ_0 and for a complete set of function $p_0(k)$.

4.2 Numerical studies. Momentum space

We have set up a program which simultaneously solves the pair of equations (29) and (30) for a given pair of initial conditions (32) by the Runge-Kutta method. For the BK evolution we have fixed the initial condition as

$$\phi_0(k) = -(1/2)\text{Ei}(-k^2/0.3657) \quad (33)$$

used in our previous calculations. We have limited our momenta in the interval $10^{-8} < k < 10^8$ and divided this interval into 1600 points.

The behaviour of $\phi(k)$ with k^2 at different values of the scaled rapidity $Y = \bar{\alpha}y = 2, 4, 6, 8$ and 10 is shown in Fig. 5. (Note that the maximal value of the scaled rapidity $Y = 10$ corresponds to the natural rapidity of order 50).

For the BFKL evolution in the external field ϕ , in the first run (A), we have taken the same form of the initial condition at $y = 0$ but with a variable slope

$$p_0(k) = -(1/2)\text{Ei}(-k^2/a). \quad (34)$$

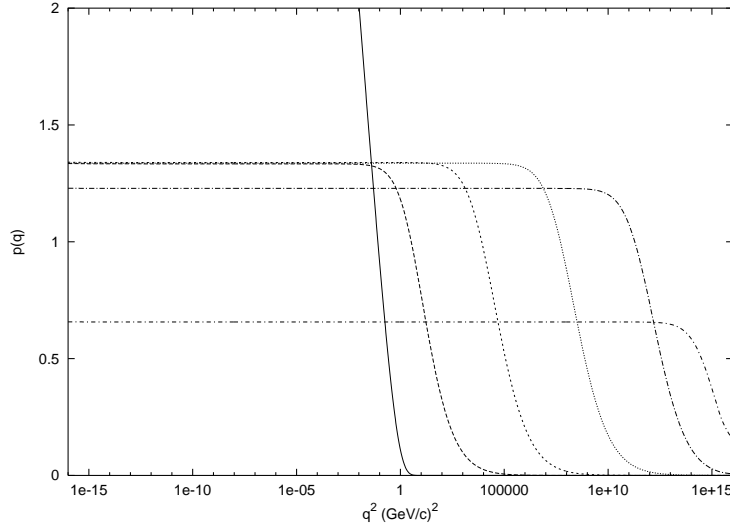


Figure 6: Solutions $p(y, q)$ of Eq. (30) as a function of q^2 for different $Y = \bar{\alpha}y$ for run A with $a = 1$. Curves which start to fall at higher q^2 correspond to higher $Y = 0, 2, 4, 6, 8$ and 10

We have performed calculations for $a = 0.2, 0.6, 1.0, 1.4$ and 1.8 . In the second run (B) the initial condition was taken with extra powers of k^2 .

$$p_0(k) = -(1/2)k^{2n}\text{Ei}(-k^2/0.3657) \quad (35)$$

with $n = 0, 1, 2, 3$ and 4 .

In all cases the behaviour of the solution $p(y, k)$ was found to be universal. At large enough y the solution becomes independent of k^2 up to a certain maximal $k_{max}^2(y)$, starting from which it goes to zero. Roughly

$$p(y, k) \sim A(y)\theta(k_{max}^2 - k^2). \quad (36)$$

As y grows $A(y)$ goes to zero and $k_{max}^2(y)$ goes to infinity. So on the whole the solution vanishes as $y \rightarrow \infty$, its x dependence tending to $\delta^2(x)$.

We illustrate this behaviour in Figs. 6 and 7, in which we show the solution $p(y, k)$ for run A with $a = 1.0$ and run B with $n = 2$ as a function of k^2 . One observes that although the values of $p(y, k)$ for the two cases are different, their behavior with y is the same: they vanish as $y \rightarrow \infty$.

This universality is especially obvious if one calculates the slope $\Delta(y, k)$ of the y -dependence of $p(y, k)$ at fixed k presenting

$$p(y, k) \propto e^{Y\Delta(y, k)}. \quad (37)$$

It turns out that at $Y > 1$ the slope $\Delta(y, k)$ is independent of k and identical for all considered cases (run A with all studied a and run B with all studied n). Its smooth behaviour with Y is shown in Fig. 8. One observes that starting from $Y = 5$ the slope becomes negative indicating that the solution goes to zero at $Y \gg 1$.

One has to take into account that in the external field $\phi(y, k)$ depending on rapidity the pomeron propagator ceases to depend only on the rapidity difference. Rather the initial and final rapidities become two independent variables. To see what influence it has on the behaviour of the propagator at large rapidities we varied the initial rapidity $y = y'$ for the evolution of $p(y, k)$, leaving unchanged the initial rapidity $y = 0$ for the evolution of $\phi(y, k)$, which is the rapidity of the nucleus. One finds

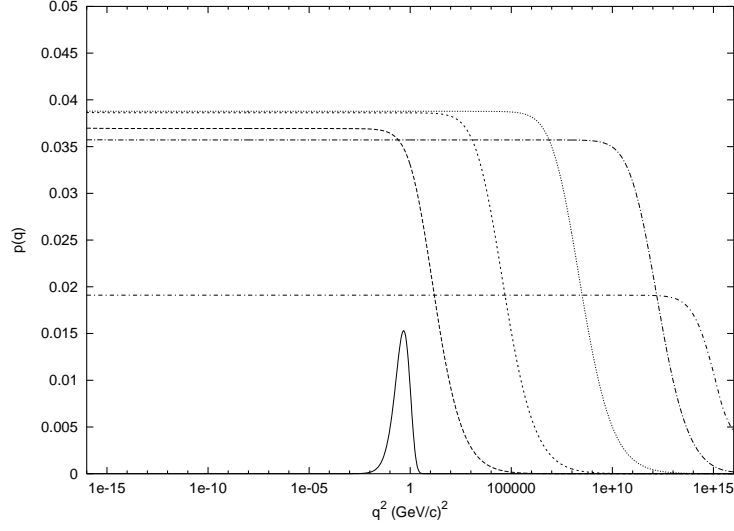


Figure 7: Solutions $p(y, q)$ of Eq. (30) as a function of q^2 for different $Y = \bar{\alpha}y$ for run B with $n = 2$. Curves which start to fall at higher q^2 correspond to higher $Y = 0, 2, 4, 6, 8$ and 10

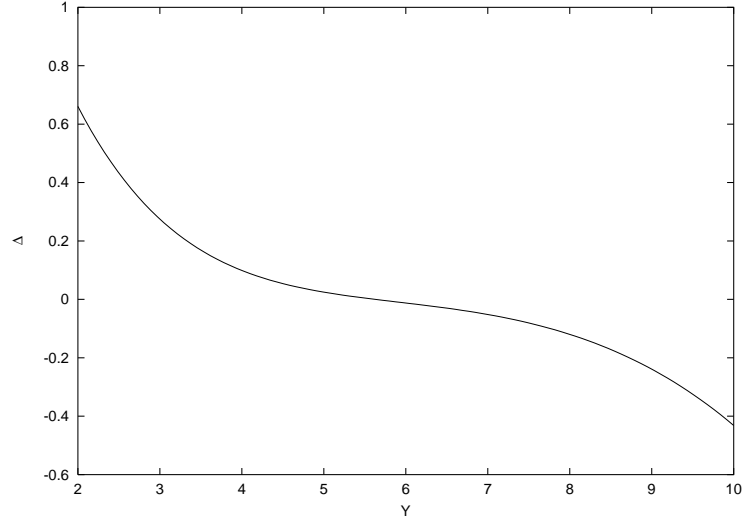


Figure 8: Slope Δ of the Y -dependence of the solutions $p(y, q)$ of Eq. (30). The slope is the same for all initial conditions (34) and (35).

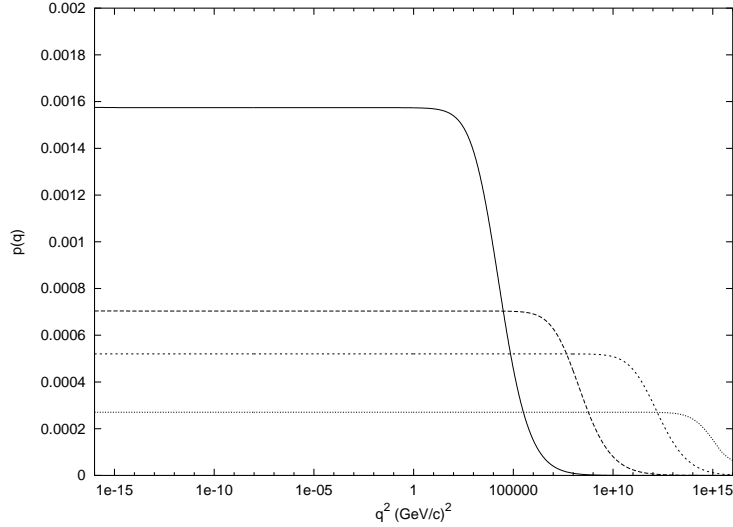


Figure 9: Solutions $p(y, q)$ of Eq. (30) as a function of q^2 for different $Y = \bar{\alpha}y$ for the initial value taken at $Y = 3$ according to run A with $a = 1$. Curves which start to fall at higher q^2 correspond to higher $Y = 4, 6, 8$ and 10

that although at initial stages of evolution the behavior of $p(y, k)$ strongly depends on the value of y' , at higher rapidities this behaviour is essentially the same for any y' , namely the convoluted propagator goes down with rapidity with the slope independent of y_0 . This is illustrated in Figs. 9 and 10 which show results for $y' = 3/\bar{\alpha}$ ($Y' = 3$) In Fig. 9 we show the solution $p(y, k)$ for run A with $a = 1$. One observes, that although absolute values of $p(y, k)$ are quite different from the case $y' = 0$ shown in Fig 6, the behaviour with the growth of rapidity is the same. It is especially clear from the values for the slope Δ shown in Fig. 10 together with those for the case $y = 0$ (Fig. 8). Again at the initial stage of the evolution the behavior with $Y' = 3$ is quite different from that with $Y_0 = 0$. However at higher rapidities the values for the slope become the same.

It is remarkable that this behaviour takes place only with ϕ given by the exact solution of the BK equation. Taking an approximate form

$$\Phi(y, x) \simeq 1 - e^{-Q^2(y)x^2}, \quad (38)$$

where the "saturation momentum" $Q^2(y) \sim e^{2.05\bar{\alpha}y}$ we obtain an equation for $p(y, k)$ in the momentum space

$$\frac{\partial p(y, k)}{\partial y} = -\bar{\alpha} \left[H_{BFKL} - \text{Ei} \left(-\frac{k^2}{4Q^2(y)} \right) \right] p(y, k). \quad (39)$$

Taking for simplicity the initial condition $p_0(k) = \phi_0(k)$ at $y = 0$ we get the solution shown in Fig. 11. One observes that at large y the solution acquires the same form (36) where however $A(y)$ grows with y :

$$A(y) \sim e^{1.4Y}. \quad (40)$$

This implies that with the approximate form (38) of Φ the final solution $P(y, x)$ in the coordinate space behaves in a singular manner at $y \rightarrow \infty$. Effectively

$$P(y, x)_{y \rightarrow \infty} \rightarrow e^{1.4y} x^2 \delta^2(x) \quad (41)$$

and it is impossible to say that it vanishes in this limit.

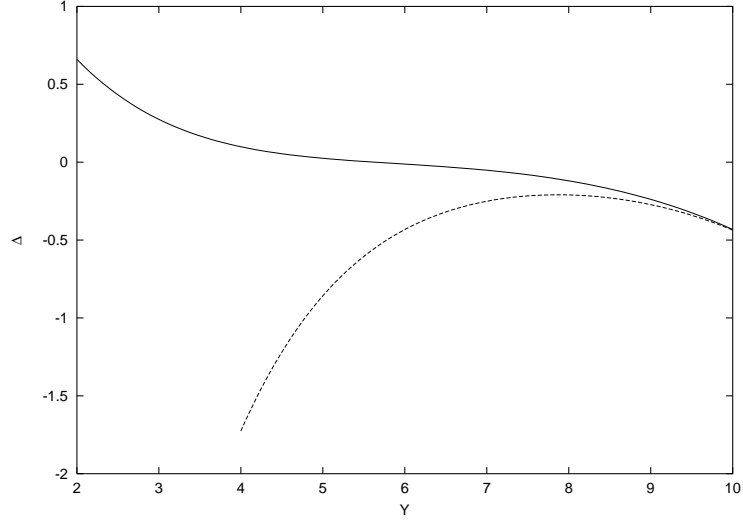


Figure 10: Slope Δ of the Y -dependence of the solutions $p(y, q)$ of Eq. (30) with the initial condition put at $Y = 0$ (upper curve) and at $Y = 3$ (lower curve) according to run A with $a = 1$.

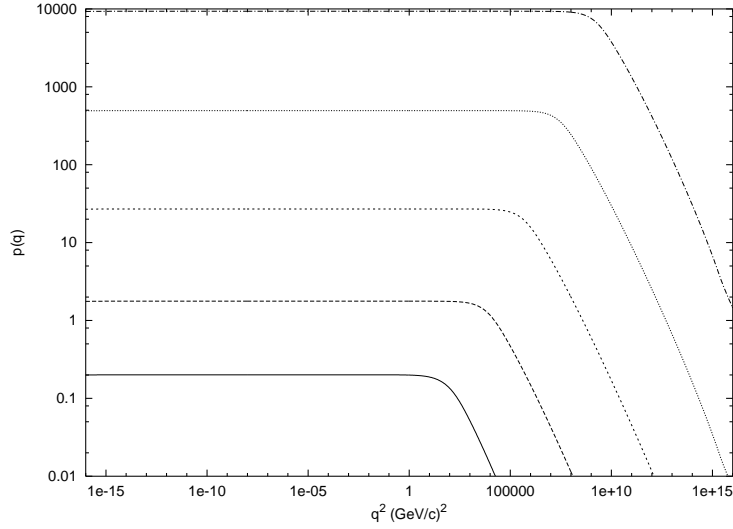


Figure 11: Solutions of Eq. (39) as a function of k^2 for different y . Curves from bottom to top correspond to $Y = \bar{\alpha}y = 2, 4, 6, 8$ and 10 .

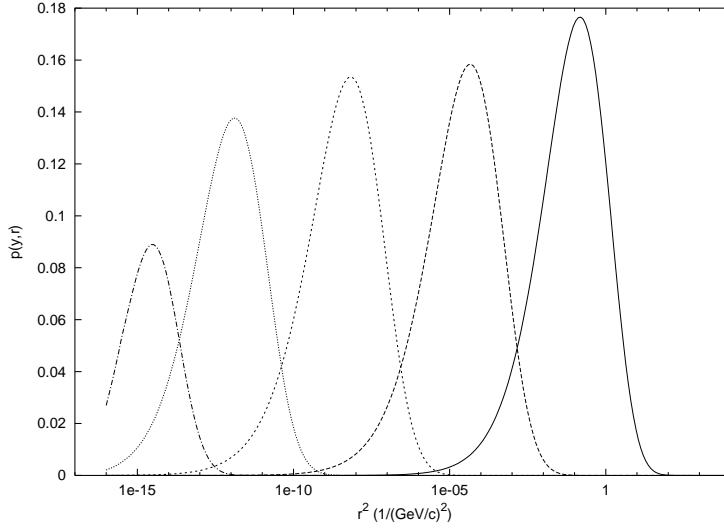


Figure 12: Solutions of Eq. (25) in the nuclear field as a function of x^2 for different y . Curves with a maximum from right to left correspond to $Y = \bar{\alpha}y = 0, 2, 4, 6, 8$ and 10 .

4.3 Numerical studies. Coordinate space

It is instructive to compare the behaviour of the propagator in the momentum space with that in the coordinate space. Rather than perform the Fourier transformation of the found propagator $p(y, k)$ and determine $P(y, x)$ according to (28) we directly solved the forward equations in the coordinate space (25) and (26) choosing the initial conditions in accordance with (33) and (34).

$$\Phi(y = 0, x) = 1 - e^{-\frac{1}{4}0.3657x^2} \quad P(y = 0, x) = 1 - e^{-\frac{1}{4}ax^2}. \quad (42)$$

Again we used the Runge-Kutta method with $10^{-8} < r < 10^8$. The number of divisions was taken 400 in $\ln r^2$ and 200 in the azimuthal angle.

Numerical calculations become much more cumbersome in the coordinate space due to the fact that the non-linear term and the term with the nuclear field depend on two different points. Having in mind that these calculations serve only for the illustrative purpose, we have restricted ourselves to only one value $a = 0.3657$ in (42), that is have taken the initial values for $P(y, x)$ at $y' = 0$ the same as for $\Phi(y, x)$. Our results are shown in Fig. 12. The form of the solution in the coordinate space very much resembles that of the gluon density in the momentum space: there is a sharp maximum at a certain value of x^2 which with the growth of y moves in the direction of smaller x^2 (to the ultraviolet). However in contrast to the gluon density the height of the maximum is diminishing with y , so that in the limit $y \rightarrow \infty$ the propagator vanishes.

In the construction of the amplitudes pomeron propagators are convoluted with the triple pomeron vertex. The behaviour of this convolution with the growth of rapidities can be studied from the integral

$$I_1(y) = \int \frac{d^2x_1 d^2x_2}{x_1^2 x_2^2} P_1(y, x_1) P_2(y, x_2) P_3(y, x_1 + x_2) \quad (43)$$

where $P_{1,2,3}$ may correspond to the same or different initial conditions. Presenting I_1 as

$$I_1(y) = a_1 e^{-\Delta_1(y)Y}, \quad y = \bar{\alpha}Y \quad (44)$$

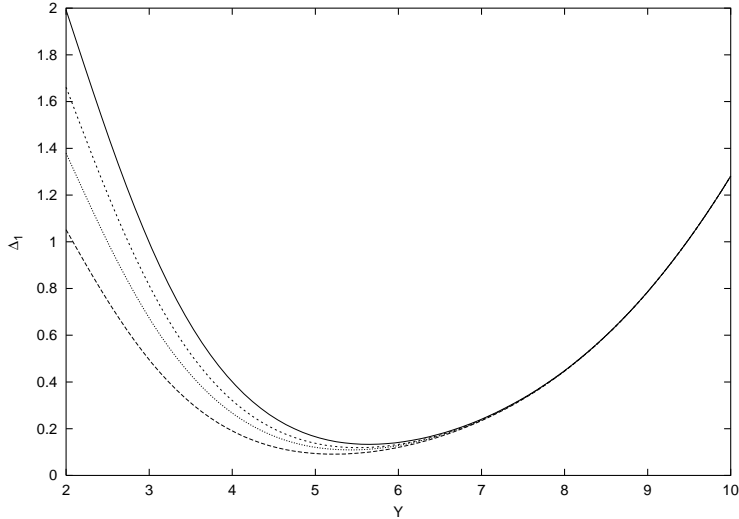


Figure 13: Exponent Δ_1 in (44) as a function of rapidity for the convolution of solutions to Eq. (25) with the initial conditions in the form (42). The curves from top to bottom correspond to 1) all three solutions with $a = 0.3657$, 2) two with $a = 0.3657$ and one with $a = 1.4$, 3) two with $a = 1.4$ and one with $a = 0.3657$ and the lowermost to all three with $a = 1.4$.

we find values of the exponent Δ_1 from our numerical calculations shown in Fig. 13 for the initial conditions (42) with $a = 0.3657$ and $a = 1.4$. As one observes, although at lower rapidities Y the values of Δ_1 depend on the choice of the initial conditions, starting from $Y = 6$ this dependence disappears and the behaviour of Δ_1 becomes universal. In any case it is clear that the convolution vanishes at $Y \rightarrow \infty$. To compare, it grows as $\exp(3\Delta_{BFKL}Y)$ in the vacuum, with $\Delta_{BFKL} = 4 \ln 2$.

5 General case

Calculations of the loop contribution require the propagator in the non-forward direction, depending not only on the relative distance between the gluons but also on the center-of mass coordinate. The convoluted propagator $P(y, r_1, r_2)$ in this case satisfies Eq. (19) with the initial condition (24). As to the nuclear field $\Phi(y, r_1, r_2)$, we may continue to consider it taken in the forward direction, neglecting the small nuclear momenta transferred to the gluons. So Φ continues to depend only on r_{12} and satisfies the same equation (26) and initial condition (42).

Propagator $P(y, r_1, r_2)$, apart from y depends on three variables for which we may take r_1^2 , r_2^2 and angle ϕ between r_1 and r_2 . We introduce a grid in variables $\ln r_1^2$, $\ln r_2^2$ and ϕ , dividing the interval in the first two variables into N_1 points and in ϕ into N_2 points. The evolution equation (19) then requires calculation of the integrand at $N_1^3 \cdot N_2^2$ points at each value of intermediate rapidities. This severely restricts the numbers of N_1 and N_2 admissible for given calculation facilities. As a result, in the past there were quite few calculations of the solution to the non-forward BK equation [19, 20] with modest values of N_1 and N_2 . In our case we use the Runge-Kutta method of the solution with the maximal value $N_1 = N_2 = 80$ compatible with the reasonable calculation time. The limits in r were taken as before $10^{-8} < r < 10^8$. The initial condition (24) for the convoluted

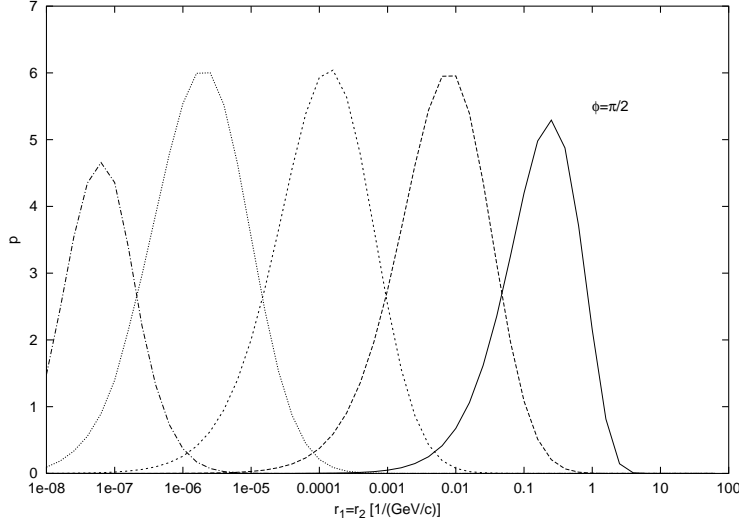


Figure 14: Propagator $P(y, r_1 = r_2, \phi = \pi/2)$ as a function of Y for the initial conditions (45) with $c_1 = 10$ and $c_2 = 2$. Curves with maxima from right to left correspond to $Y = 2, 4, 6, 8, 10$ respectively.

propagator was taken at $y' = 0$ in the form borrowed from [19]

$$P(y = 0, r_1, r_2) = 1 - e^{-c_1 r_{12}^2 e^{-b^2/c_2}}, \quad (45)$$

where $b = (r_1 + r_2)/2$. We have studied 9 cases with $c_1 = 0.1, 1$ and 10 and $c_2 = 0.2, 2$ and 20 . In all cases the results are quite similar.

Calculations produce an array of data $P(y, r_1^2, r_2^2, \phi)$ on the three-dimensional grid. The results can be presented in various ways. In Fig. 14 we show values of $P(y, r_1^2, r_2^2, \phi)$ with $c_1 = 10$ and $c_2 = 2$ at $r_1 = r_2$ and $\phi = \pi/2$ for different y .

As we see the general trend of the curves is the same as for the forward case, Fig 12, although the decrease of the height of the maximum starts from larger rapidities. The behaviour of $P(y, r_1 = r_2, \phi)$ at different values of ϕ and for different c_1 and c_2 in the initial conditions (24) is the same, although the value of the rapidity Y at which the decrease starts is slightly different for different initial conditions.

To have an overall picture of the behaviour of the non-forward propagator with rapidity, as for the forward case, we studied the convolution of three propagators with the triple pomeron vertex (dropping operator K , which hopefully does not change the behaviour at large y , see [8])

$$I_2(y) = \int \frac{d^2 r_1 d^2 r_2 d^2 r_3}{r_{12}^2 r_{23}^2 r_{31}^2} P_1(y, r_1, r_2) P_2(y, r_2, r_3) P_3(y, r_3, r_1), \quad (46)$$

where P_1 , P_2 and P_3 may come from the same or different initial conditions. We again present

$$I_2(y) = a_2 e^{-\Delta_2(y)Y}, \quad y = \bar{\alpha}Y \quad (47)$$

and in Fig. 15 show values of $\Delta_2(y)$ for four cases, with the three propagators taken 1) all for the initial condition (IC) with $c_1 = 10$, $c_2 = 2$ (IC=A) 2) all for the IC with $c_1 = 1$, $c_2 = 20$ (IC=B) 3) two propagators with IC=A and one with IC=B and 4) two propagators with IC=B

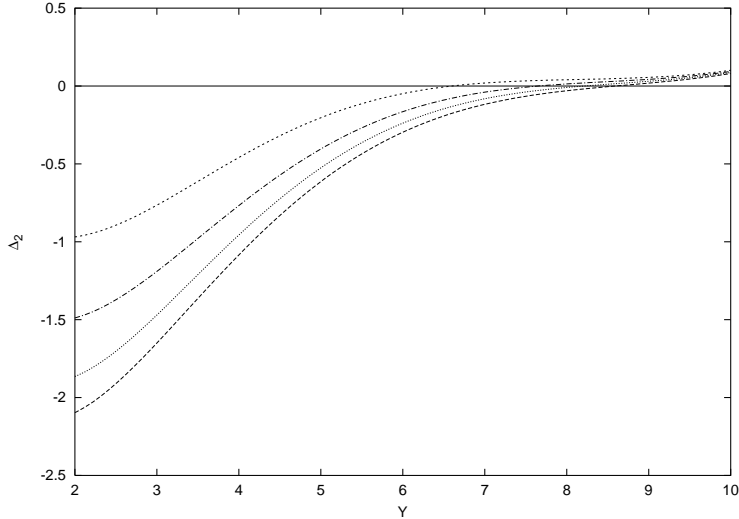


Figure 15: Exponent Δ_2 in (46) as a function of rapidity for the convolution of solutions to Eq. (19) with the initial conditions (IC) A and B in (45)(see explanation in the text. The curves from top to bottom correspond to 1) all three solutions with IC=A 2) two with IC=A and one with B 3) two with IC= B and one with A and the lowermost to all three solutions with IC=B

and one with IC=A. We see that at low values of Y the exponents Δ_2 are different for these cases and predominantly negative, which means that the propagators in fact grow at these rapidities. However at larger rapidities different Δ_2 converge to a common positive value indicating that the convolution decreases with rapidity and that this decrease is universal.

6 Conclusions

We have studied numerically the BFKL pomeron propagator in the external field created by the solution of the BK equation in the nuclear matter. We have found that for more or less arbitrary set of initial conditions the convoluted propagator vanishes at large rapidities, its coordinate dependence in the forward case tending to the δ -function. This gives reasons to believe that the propagator itself vanishes at large rapidities in the nuclear background. This result follows only with the field being the exact solution of the BK equation.

Our results may be a starting point for the perturbative calculation of loop contributions in the nuclear background. However the technical difficulties seem to be quite formidable, since calculations are only possible numerically and even simplest loops involve quite a number of spatial points over which one has to integrate. One needs to invent a reliable approximate representation for the non-forward propagator in the nuclear field which would allow one to perform all these integrations effectively. A somewhat simpler application is to the study of double inclusive cross-section for gluon jet production in nucleus-nucleus collisions, which only requires the forward propagator. Both these complicated problems are left for future investigations.

7 Acknowledgments

The authors are indebted to J.Bartels, E.Levin, L.Lipatov and A.Mueller for discussion. This work has been supported by grants RFFI 09-012-01327-a and RFFI-CERN 08-02-91004. A.T. also acknowledges the FTP "Scientific and scientific-pedagogical personnel of innovative Russia in 2009-2013" (Contract No. P20).

References

- [1] I.I.Balitsky, Nucl. Phys. **B 463** (1996) 99.
- [2] Yu.V.Kovchegov, Phys. Rev **D 60** (1999) 034008; **D 61** (2000) 074018.
- [3] M.A.Braun, Eur. Phys. J. **C 16** (2000) 337.
- [4] M.A.Braun, Phys. Lett. **B 483** (2000) 115.
- [5] M.A.Braun, Phys. Lett. **B 632** (2006) 297.
- [6] R.Peschansky, Phys. Lett. **B 109** (1997) 491.
- [7] J.Bartels, M.Ryskin, G.P,Vacca Eur. Phys. J. **C 27** (2003) 101.
- [8] M.A.Braun, Eur. Phys. J. **C 63** (2009) 287.
- [9] E.Iancu, D.N.Triantafyllopoulos, Nucl. Phys, **A 756** (2005) 419.
- [10] A.H.Mueller, A.I.Shoshi, S.M.N.Wong , Nucl. Phys. **B 715** (2005) 440.
- [11] E.Levin, M.Lublinsky, Nucl. Phys. **A 763** (2005) 172.
- [12] E.Levin, Nucl. Phys. **A 763** (2005) 740.
- [13] C.Marquet, R.Peschansky, G.Soyez, Phys. Rev. **D 73** (2006) 114005.
- [14] E.Levin, J.Miller, A.Prygarin, Nucl. Phys. **A 806** (2008) 254.
- [15] G.Soyez, Acta Phys. Polon **B 37** (2006) 3477.
- [16] M.A.Braun and A.Tarasov, Eur. Phys. J **C 58** (2008) 383.
- [17] A.Schwimmer, Nucl.Phys. **B 94** (1975) 445.
- [18] L.N.Lipatov, in *Perturbative QCD*, ed. by A.H.Mueller (world Scientific, Singapore, 1989).
- [19] K.Golec-Biernat and A.M.Stasto, Nucl. Phys. **B 668** (2003) 345.
- [20] J.Berger and A.M.Stasto, arXiv: 1010.0671.